NASA/TM—20220007239

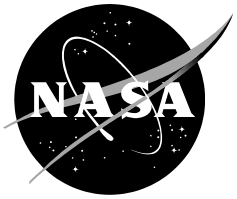

Si5345, SY88422L, LT3482, and MSK130 components Total Ionizing Dose Test Report

Jonathan D. Barth

Landen D. Ryder

Rebekah A. Austin

May 2022

NASA STI Program Report Series

The NASA STI Program collects, organizes, provides for archiving, and disseminates NASA's STI. The NASA STI program provides access to the NTRS Registered and its public interface, the NASA Technical Reports Server, thus providing one of the largest collections of aeronautical and space science STI in the world. Results are published in both non-NASA channels and by NASA in the NASA STI Report Series, which includes the following report types:

- TECHNICAL PUBLICATION. Reports of completed research or a major significant phase of research that present the results of NASA Programs and include extensive data or theoretical analysis. Includes compilations of significant scientific and technical data and information deemed to be of continuing reference value. NASA counterpart of peer-reviewed formal professional papers but has less stringent limitations on manuscript length and extent of graphic presentations.

- TECHNICAL MEMORANDUM. Scientific and technical findings that are preliminary or of specialized interest, e.g., quick release reports, working papers, and bibliographies that contain minimal annotation. Does not contain extensive analysis.

- CONTRACTOR REPORT. Scientific and technical findings by NASA-sponsored contractors and grantees.

- CONFERENCE PUBLICATION. Collected papers from scientific and technical conferences, symposia, seminars, or other meetings sponsored or co-sponsored by NASA.

- SPECIAL PUBLICATION. Scientific, technical, or historical information from NASA programs, projects, and missions, often concerned with subjects having substantial public interest.

- TECHNICAL TRANSLATION. English-language translations of foreign scientific and technical material pertinent to NASA's mission.

Specialized services also include organizing and publishing research results, distributing specialized research announcements and feeds, providing information desk and personal search support, and enabling data exchange services.

For more information about the NASA STI program, see the following:

- Access the NASA STI program home page at http://www.sti.nasa.gov

- Help desk contact information:

https://www.sti.nasa.gov/sti-contact-form/ and select the "General" help request type.

NASA/TM—20220007239

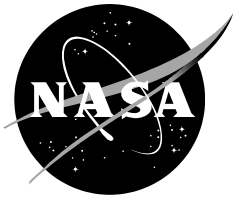

Si5345, SY88422L, LT3482, and MSK130 components Total Ionizing Dose Test Report

Jonathan D. Barthr
Goddard Space Flight Center, Greenbelt, MD

Landen D. Ryder
Goddard Space Flight Center, Greenbelt, MD

Rebekah A. Austin
Goddard Space Flight Center, Greenbelt, MD

Test Start Date: 7/21/2021
Test Completion Date: 7/23/2021
Test Report Date: 12/6/2021

National Aeronautics and
Space Administration

Goddard Space Flight Center
Greenbelt, MD 20771

May 2022

Acknowledgments

This work was sponsored by the NASA GSFC Radiation Effects and Analysis Group and supported by the Combined Science and Navigation Lidar for CAESAR New Frontiers 5 Internal Research & Development Program (IRAD), Comet Astrobiology Exploration SAmple Return (CAESAR) project.

Level of Review: This material has been technically reviewed by technical management.

Available from

NASA STI Program
Mail Stop 148
NASA's Langley Research Center
Hampton, VA 23681-2199

National Technical Information Service
5285 Port Royal Road
Springfield, VA 22161
703-605-6000

This report is available in electronic form at

https://radhome.gsfc.nasa.gov/

TABLE OF CONTENTS

1. Introduction 3
2. Devices Tested 3
   2.2. Device Under Test (DUT) Information 4
Table 1. Si5345 Information 4
Table 2. SY88422L Information 5
Table 3. LT3482 Information 6
Table 4. MSK130 Information 7
3. Test Description 7
   3.1. Test Setup 7
   3.2. Irradiation Conditions 9
4. Failure Criteria 9
5. Results 10
   5.1. Si5345 10
   5.2. SY88422L 17
   5.3. MSK130 21
   5.4. LT3482 24
6. Summary 25
7. References 25

1. INTRODUCTION

The purpose of this test was to characterize the SI-5345, SY88422L, LT3482 and MSK130 parameter degradation for total dose response. The components are associated with REAG ID #21-024. In the test, each device was exposed to high dose rate (HDR) irradiation using gamma radiation. Device parameters such as leakage currents, timing, and overall chip health were investigated. These devices were tested for an interstellar mission on a trajectory between 0.9 AU and 5.3 AU with a 2.5-year mission, yielding an expected overall dose of 29 krad(Si)behind 1 mm of aluminum shielding (at 95% confidence; environment and dose determined through SPENVIS).

This test report gives an initial look at candidate parts. Extremely small sample sizes (only 1 or 2 devices tested) do not allow consideration of part-to-part variability. High dose rates were used despite LT3482 and MSK130 having potential enhanced low dose rate sensitivity (ELDRS). Care should be taken in interpreting results given these limitations.

2. DEVICES TESTED

2.1. Part Background

Si5345

The Skyworks Si5345 is a jitter attenuating clock multiplier. The Si5345's internal DSPLL (Digital Phase Locked Loop) provides jitter attenuation and any-frequency multiplication of the selected input frequency. Fractional input dividers (P) allow the DSPLL to perform hitless switching between input clocks (INx) that are fractionally related. Input switching is controlled manually or automatically using an internal state machine. The oscillator circuit (OSC) provides a frequency reference which determines output frequency stability and accuracy while the device is in free-run or holdover mode. The high-performance MultiSynth dividers (N) generate integer or fractionally related output frequencies for the output stage. A crosspoint switch connects any of the MultiSynth generated frequencies to any of the outputs. Additional integer division (R) determines the final output frequency.

SY88422L

The Microchip SY88422L is a single 3.3 V supply, small form factor laser driver for telecom/datacom applications up to 4.25 Gbps. The driver can deliver modulation current up to 90mA and a bias current up to 100 mA.

LT3482

The Analog Devices LT3482 is a fixed frequency current mode step-up DC/DC converter with voltage doubler designed to bias avalanche photodiodes (APDs) in optical receivers. It can provide up to 90 V output. The LT3482 features high side APD bias current monitoring with better than 10% relative accuracy over the entire temperature range. An integrated high side current monitor produces a current proportional to APD bias current with better than 10% relative accuracy over four decades of dynamic range in the input range of 250nA to 2.5mA. This APD bias current can be used as a reference to provide a digitally programmed output voltage via the CTRL pin.

MSK130
The MS Kennedy MSK130 is a high speed, high voltage differential amplifier designed for output currents up to ±200 mA and utilizes external compensation.

2.2. Device Under Test (DUT) Information

2.2.1. Si5345

Two Si5345 clock synthesizers were tested. One control was used. All specifications and descriptions are according to the datasheet [1]. More information can be found in Table 1. Pinout information for Si5345 can be seen in Figure 1.

Table 1. Si5345 Information

Part Number	Si5345
Manufacturer	Silicon Labs/SkyWorks
Lot Date Code	n/a
Additional Case Markings	SI5345-D-EVB
Quantity Tested	2 DUTs, 1 control
Part Function	Clock Synthesizer
Part Technology	Si CMOS
Package	64-Pin QFN

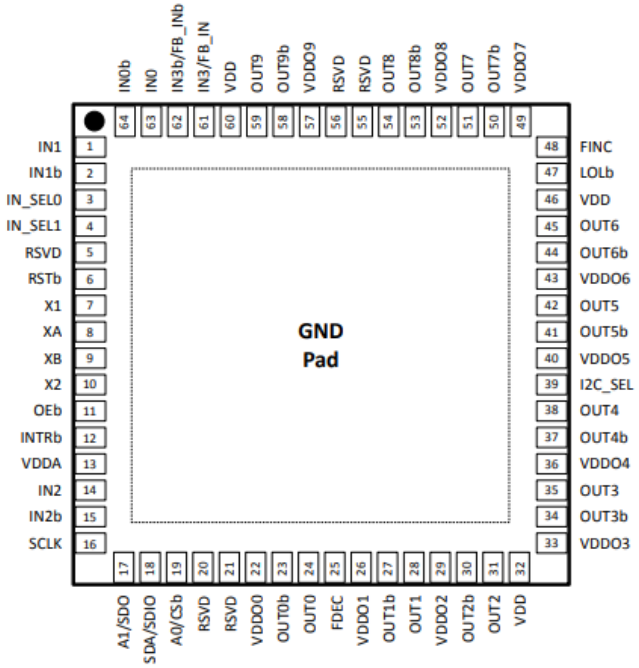

Figure 1: Pinout of Si5345

2.2.2. SY88422L

Two SY88422L laser drivers were tested. One control was used. All specifications and descriptions are according to the datasheet [2]. More information can be found in Table 2. Pinout information for SY88422L can be seen in Figure 2.

Table 2. SY88422L Information

Part Number	SY88422L
Manufacturer	Microchip
Lot Date Code	n/a
Additional Case Markings	n/a
Quantity Tested	2 DUTs, 1 control
Part Function	Laser Driver
Part Technology	SiGe Bipolar
Package	16-Pin QFN

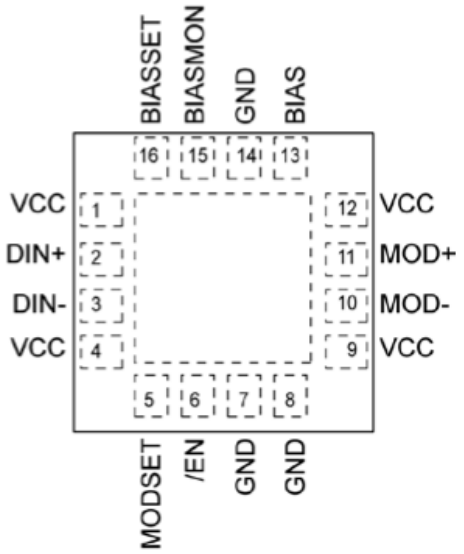

Figure 2: Pinout of SY88422L

2.2.3. LT3482

One LT3482 DC/DC Converter was tested. No control was used. All specifications and descriptions are according to the datasheet [3]. More information can be found in Table 3. Pinout information for LT3482 can be seen in Figure 3.

Table 3. LT3482 Information

Part Number	LT3482
Manufacturer	Analog Devices
Lot Date Code	n/a
Additional Case Markings	n/a
Quantity Tested	1
Part Function	DC/DC Converter
Part Technology	Si Bipolar
Package	16-Pin QFN

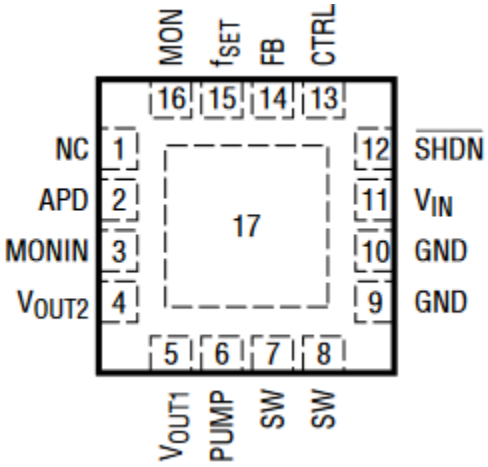

Figure 3: Pinout LT3482

2.2.4. MSK130

One MSK130 Differential Amplifier was tested. No control was used. All specifications and descriptions are according to the datasheet [4]. More information can be found in Table 4. Pinout information for MSK130 can be seen in Figure 4.

Table 4. MSK130 Information

Part Number	MSK130
Manufacturer	M.S. Kennedy, TTM Technologies
Lot Date Code	n/a
Additional Case Markings	n/a
Quantity Tested	1
Part Function	Differential Amplifier
Part Technology	BiCMOS
Package	10-Pin SIP

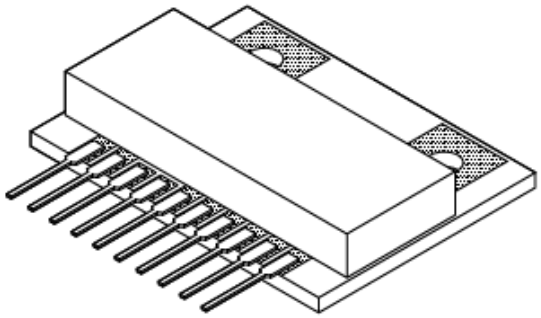

PIN-OUT INFORMATION

1	-Input	10	Output
2	+Input	9	Comp2
3	No Connection	8	Comp1
4	No Connection	7	Isense
5	-Vcc	6	+Vcc

Figure 4: Pinout of MSK130

3. TEST DESCRIPTION

3.1. Test Setup

Tests were conducted using MIL-STD-883, Method 1019 as guidance. Electrostatic discharge (ESD) procedures were followed during test and transfer of the devices between irradiation chamber and characterization. Exposures were performed at ambient laboratory temperature.

Note: the Si5345 was tested on evaluation board part number SI5345-D-EVB. To constrain testing to Si5345, support components on the board were shielded with approximately 4 inches of lead, resulting in a reduction of ~99.6% over the TID delivered to the DUT. Both SI5345-D-EVB boards were irradiated individually due to the nature of the radiation field within the collimated chamber.

Test setups for each of the part types irradiated and their bias conditions are shown in Figure 5, Figure 6, and Figure 7. Test equipment was provided and run by Xiaoli Sun and Jacob Hwang. Additional details are provided in the Results section 5. Note that a multi-channel power supply was used to provide two distinct voltage channels to the LT3482 and MSK130 devices during testing.

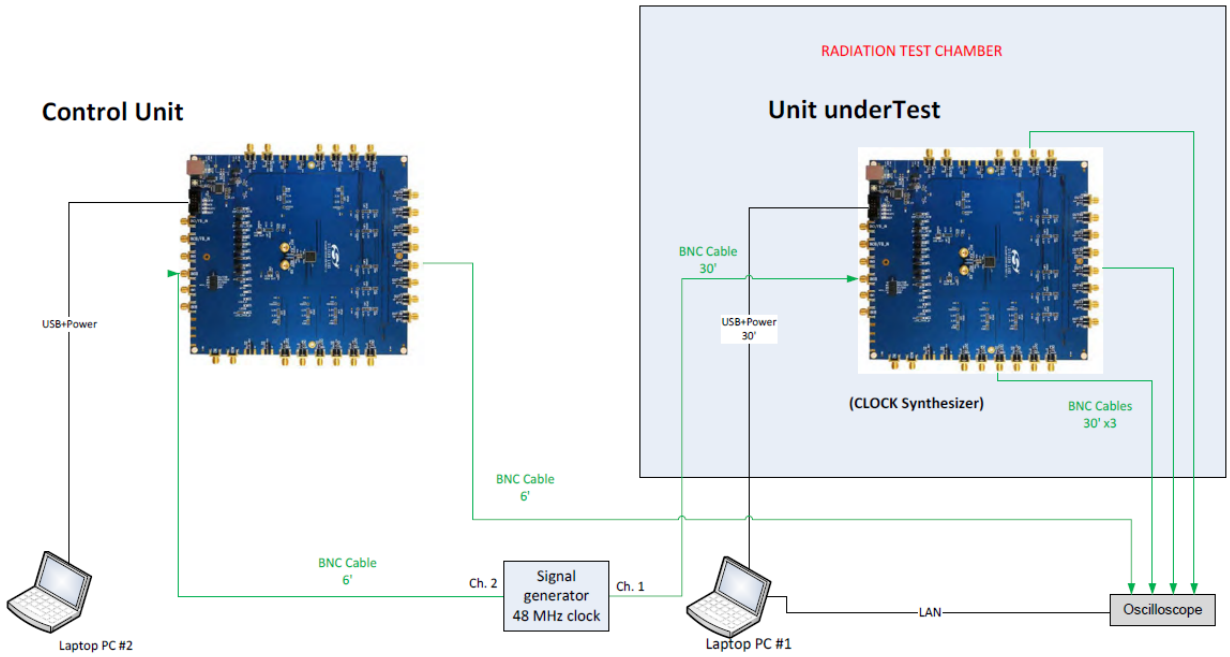

Figure 5: Si5345 test setup on board SI5345-D-EVB

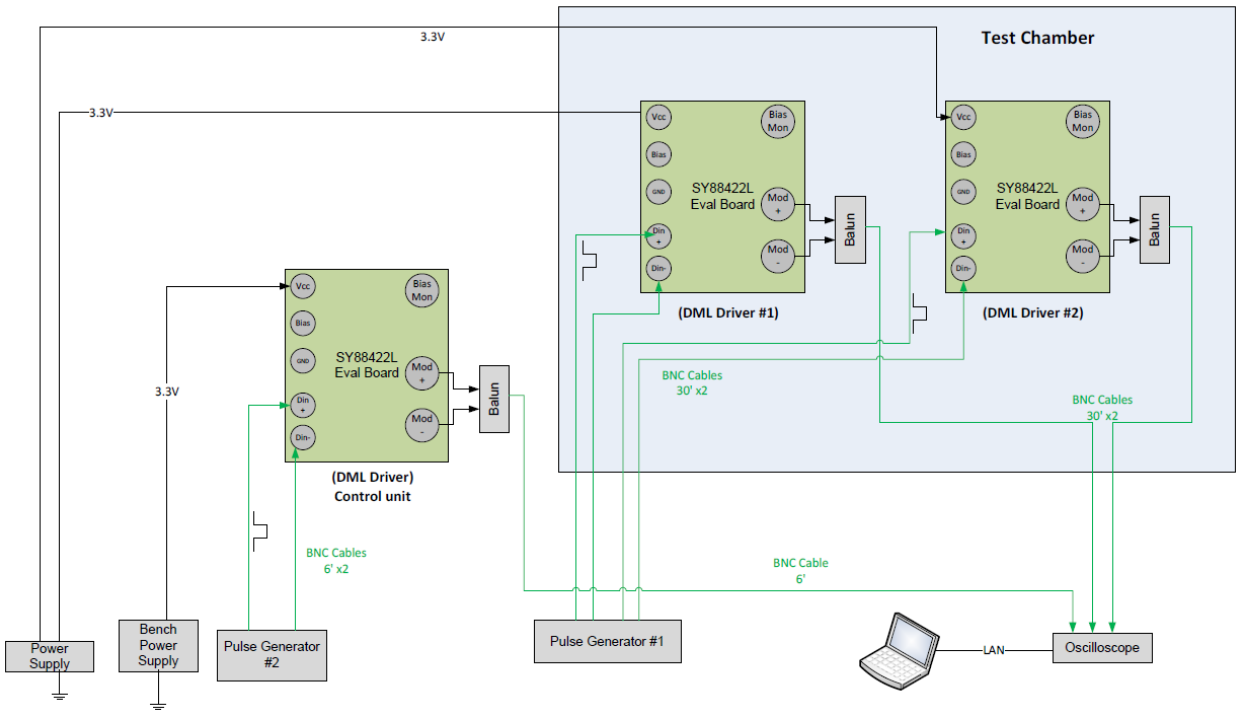

Figure 6: SY88422L test setup

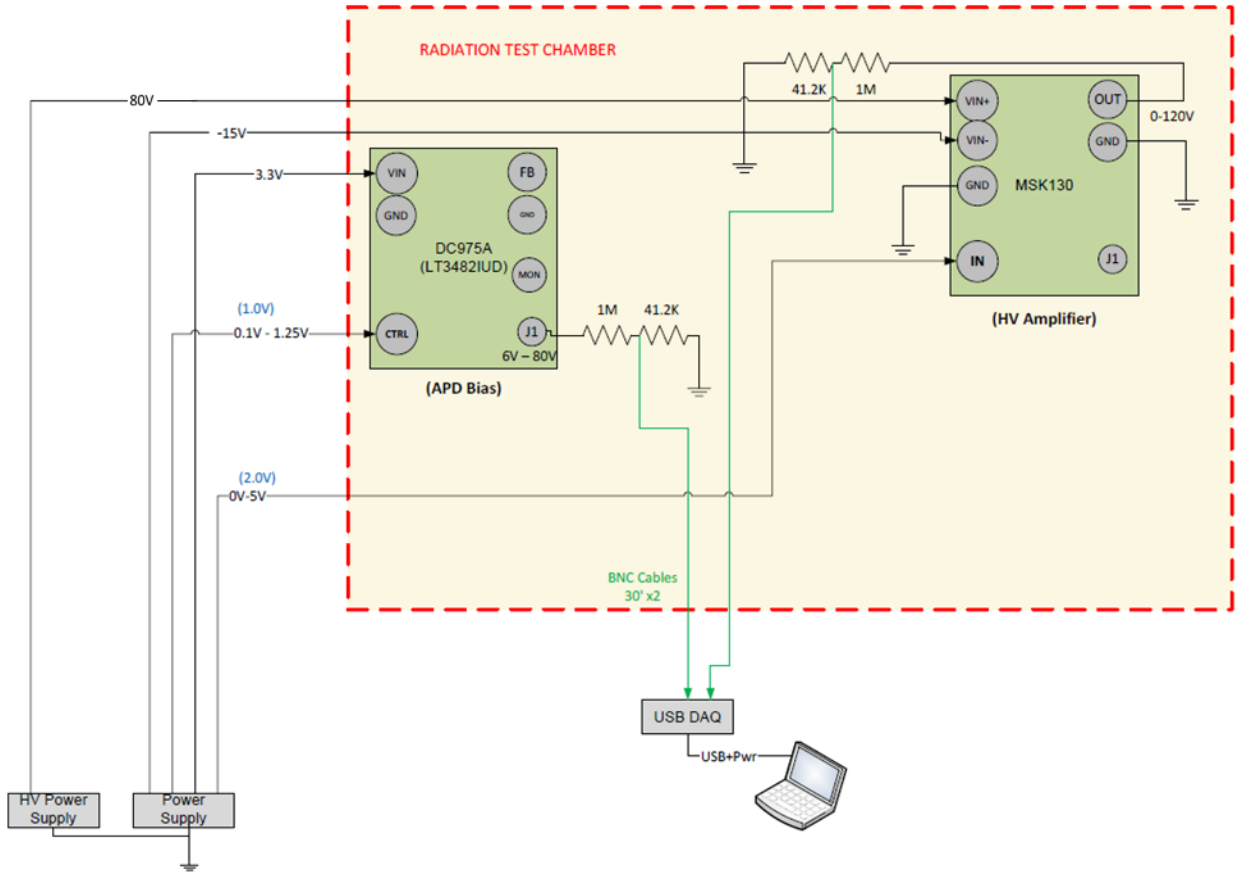

Figure 7: LT3482 and MSK130 setup

3.2. Irradiation Conditions

Testing was done at room temperature in a room air source gamma ray facility, which is compliant with MIL-STD-883, Method 1019. Dosimetry is National Institute of Standards and Technology (NIST) traceable. Parts were placed in a Pb/Al box and exposed under biased condition to ~1 MeV gamma radiation at a high dose rate. Prior to the first radiation dose, all parts were electrically tested and programmed. After each exposure level, the DUTs and controls were electrically characterized again. The DUTs were re-exposed to radiation within the time limits defined by MIL-STD-883, Method 1019 when possible.

Each part type was irradiated under bias to dose steps of 1k, 2k, 5k, 10k, 20k, 50k, 75k, and 100k rad(Si). Dose rate for the Si5345 was 0.562 krad(Si)/min; SY88422L, LT3482 and MSK130 were exposed at 1.190 krad(Si)/min.

4. Failure Criteria

Because this testing was characterizing possible parts for a research program, no failure criteria were prescribed.

5. RESULTS

5.1. Si5345

Three SI5345 devices (one control and two irradiated DUTs) were powered using USBs connected to a laptop; lead blocks were configured in manner that shielded the sensitive support circuitry on the evaluation board during irradiation. A 48 MHz signal was supplied as an input clock signal to both the control and irradiated boards through a function generator connected with 6 ft and 30 ft BNC cables respectively. Internal voltage monitors on the Si5345 devices allow monitoring during irradiation of the on-chip supply voltages of each channel through the USB connected laptop running manufacturer-provided software. To monitor for radiation-induced timing degradation the output waveforms from both the control and irradiated devices were monitored using an oscilloscope through 6 ft and 30 ft BNC cables respectively.

Internal supply current and voltage as a function of dose for both irradiated devices are provided in Figures 8-17. Although the current remained consistent, there is a slight decrease in the voltage as a function of dose on the output channels (~1%). To examine potential radiation-induced degradation on the timing response of the devices, output waveforms from multiple output channels prior to irradiation and after 100 krad(Si) are provided in Figures 18-21. Note that the reference waveforms correspond to the output channel of the control device and the timing offset is likely due to differences in cabling lengths. The waveforms remain consistent, showing minimal if any radiation-induced degradation in the timing (the vertical shift observed in channel 6 of DUT 1 is a consequence of erroneous oscilloscope settings).

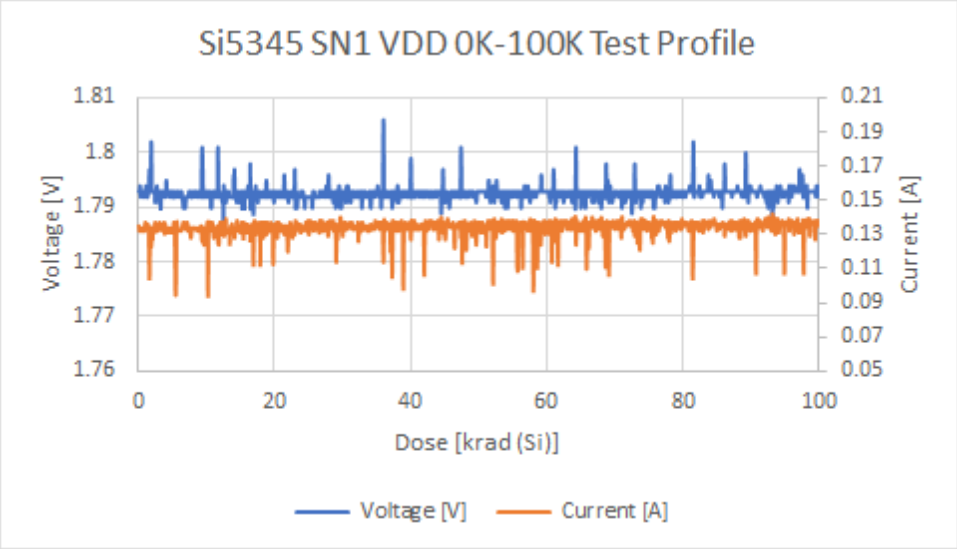

Figure 8: Internal voltage and current of the VDD port as a function of dose for Si5345 DUT 1.

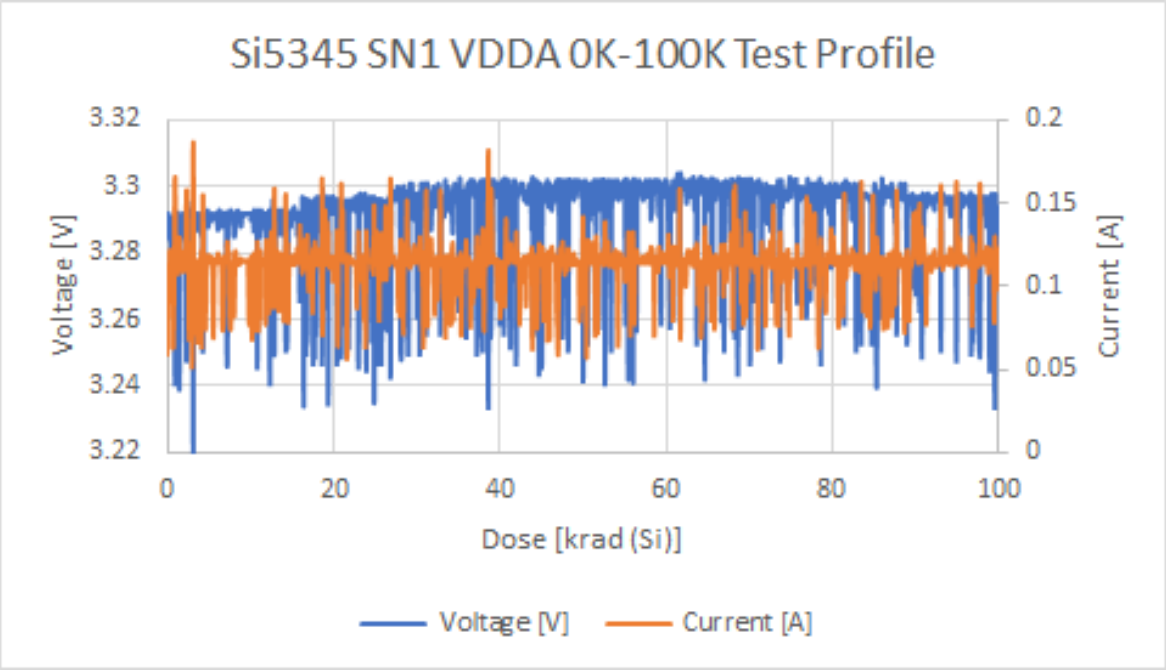

Figure 9: Internal voltage and current of the VDDA port as a function of dose for Si5345 DUT 1.

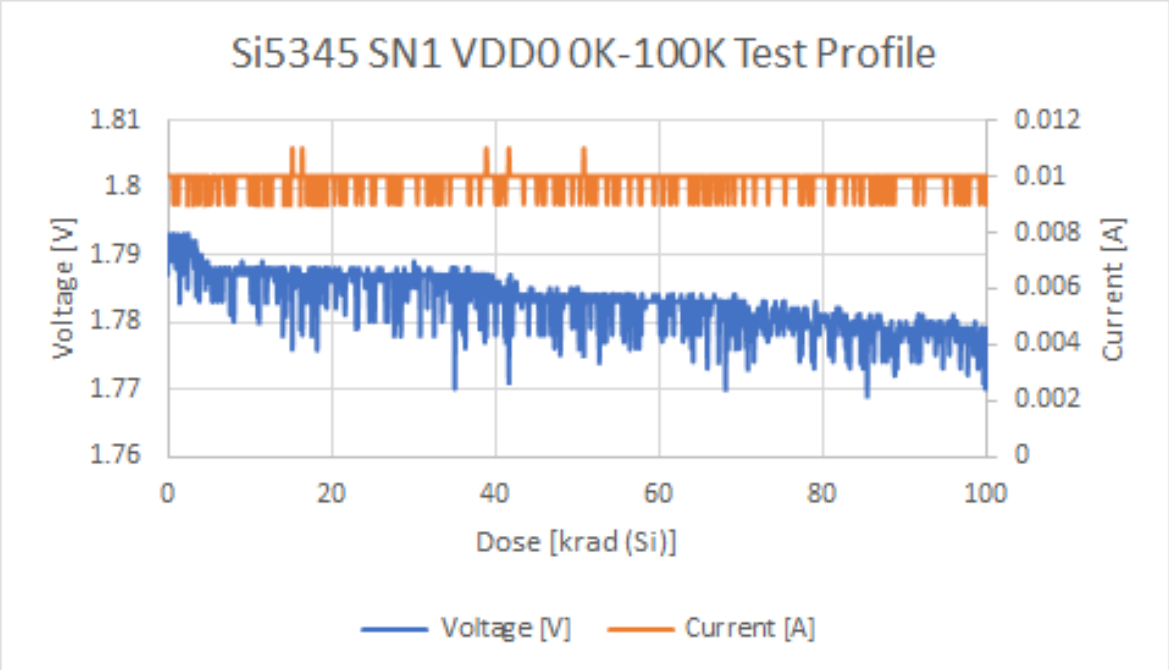

Figure 10: Internal voltage and current of the VDD0 port as a function of dose for Si5345 DUT 1.

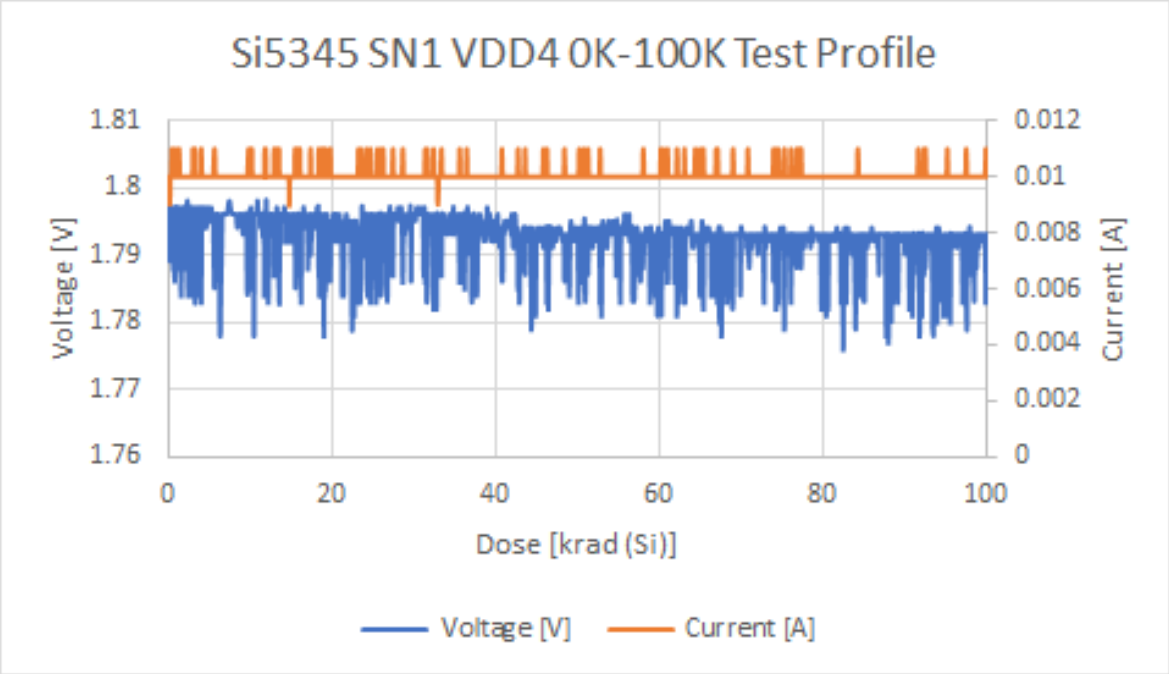

Figure 11: Internal voltage and current of the VDD4 port as a function of dose for Si5345 DUT 1.

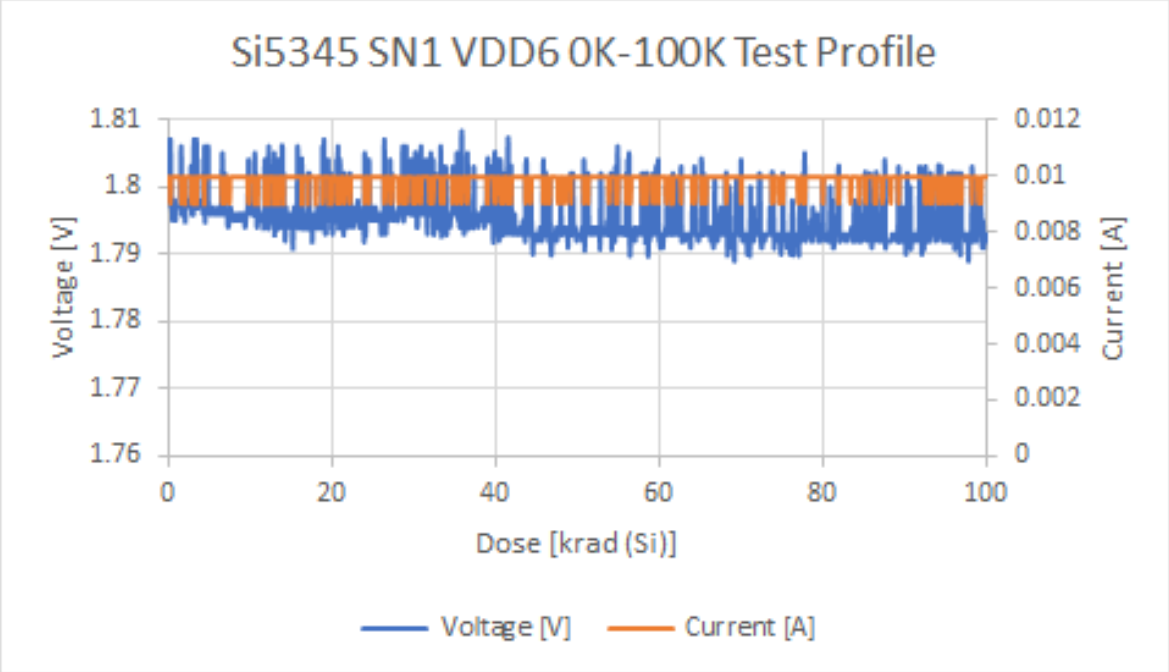

Figure 12: Internal voltage and current of the VDD6 port as a function of dose for Si5345 DUT 1.

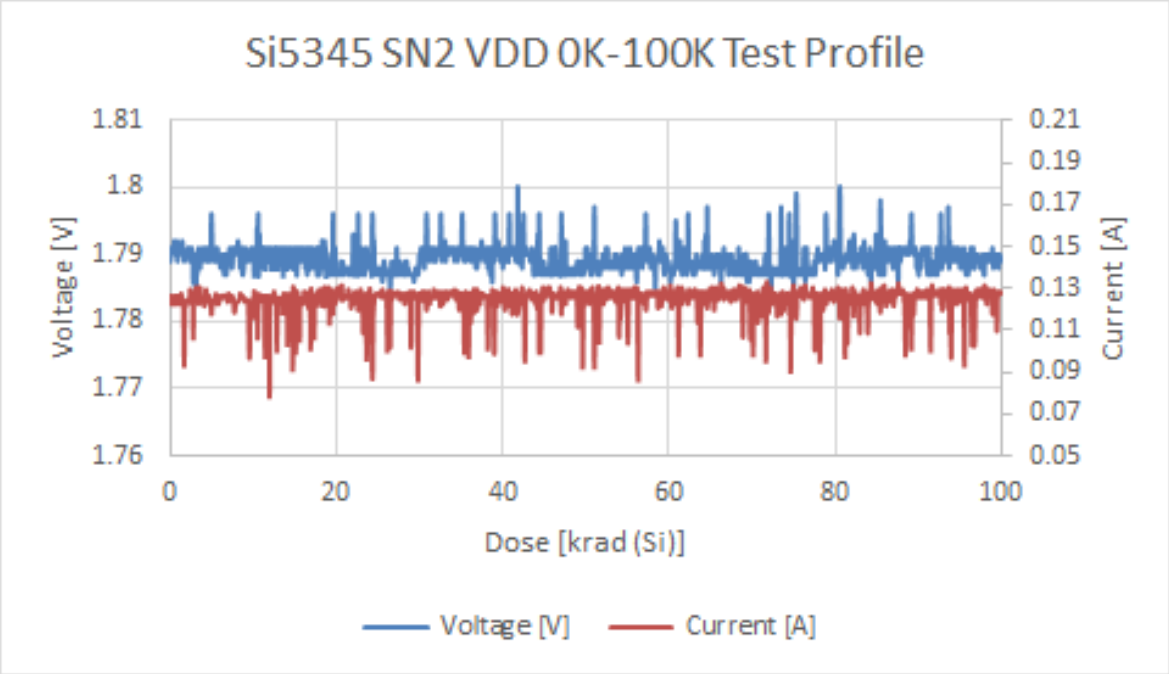

Figure 13: Internal voltage and current of the VDD port as a function of dose for Si5345 DUT 2.

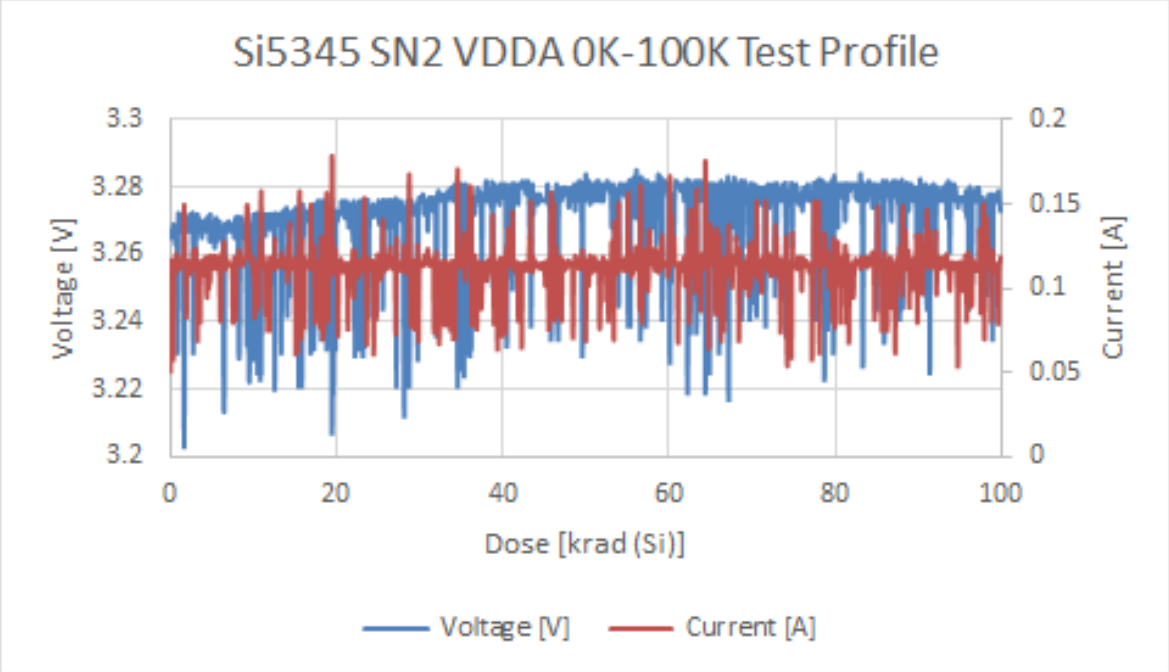

Figure 14: Internal voltage and current of the VDDA port as a function of dose for Si5345 DUT 2.

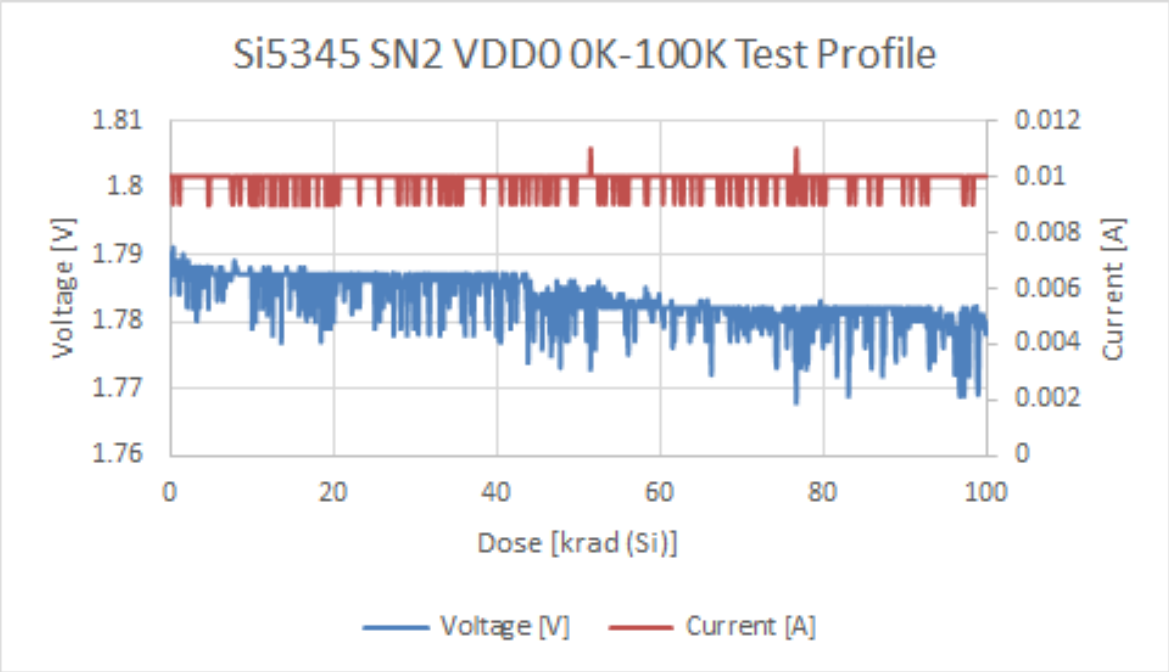

Figure 15: Internal voltage and current of the VDD0 port as a function of dose for Si5345 DUT 2.

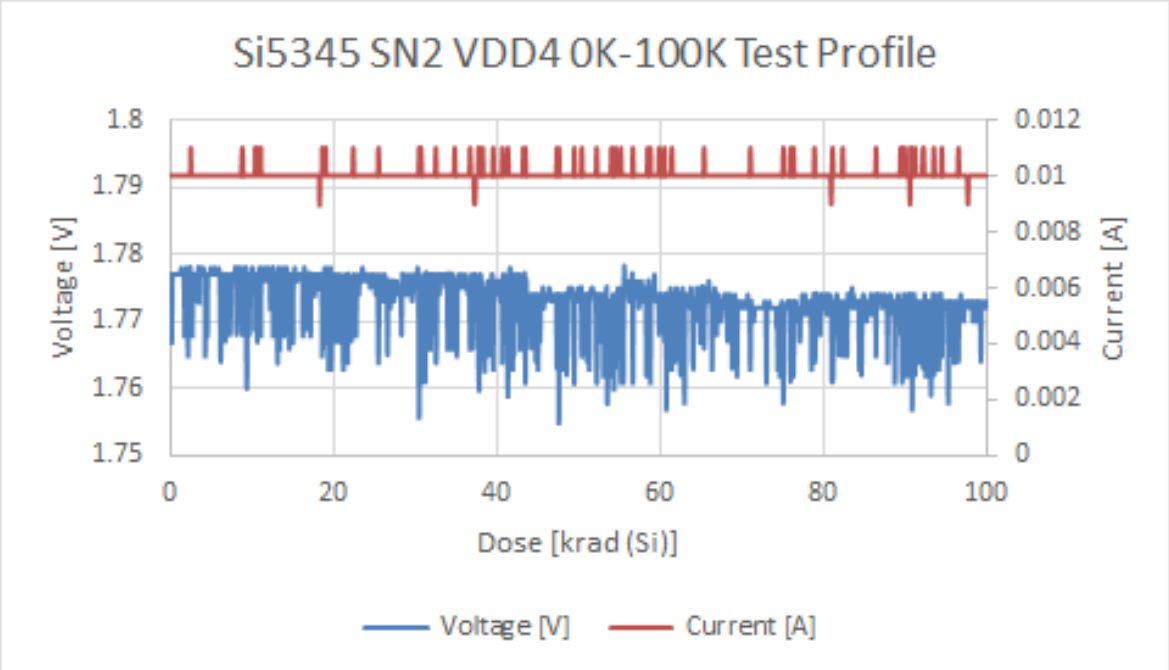

Figure 16: Internal voltage and current of the VDD4 port as a function of dose for Si5345 DUT 2.

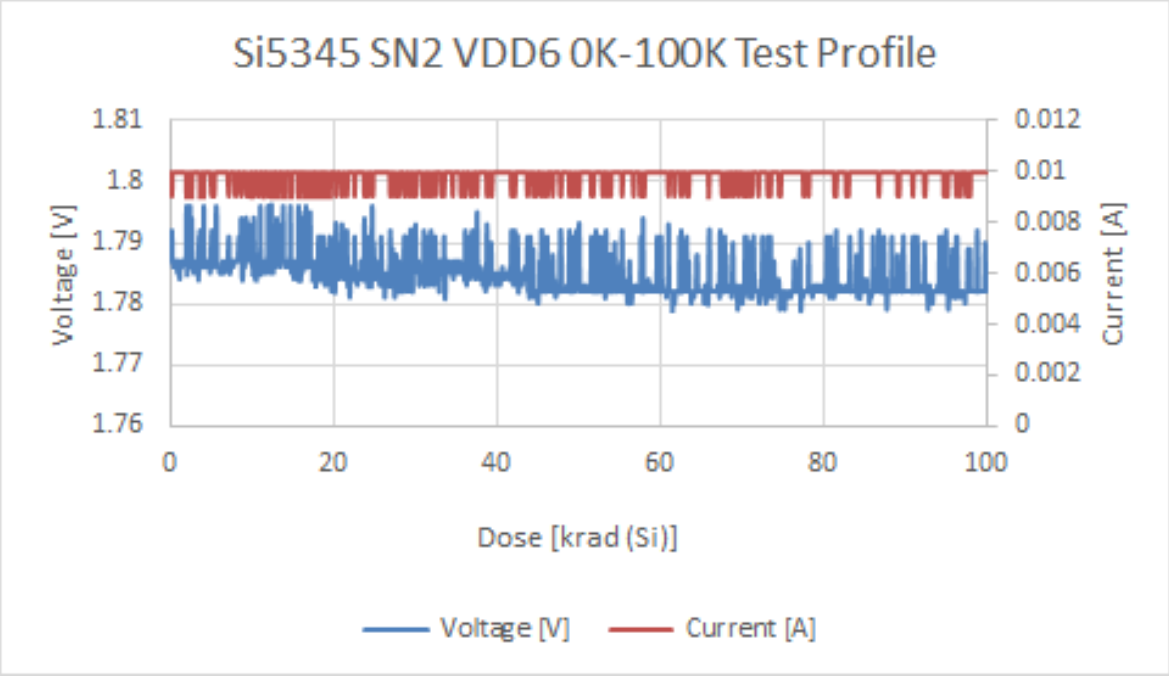

Figure 17: Internal voltage and current of the VDD6 port as a function of dose for Si5345 DUT 2.

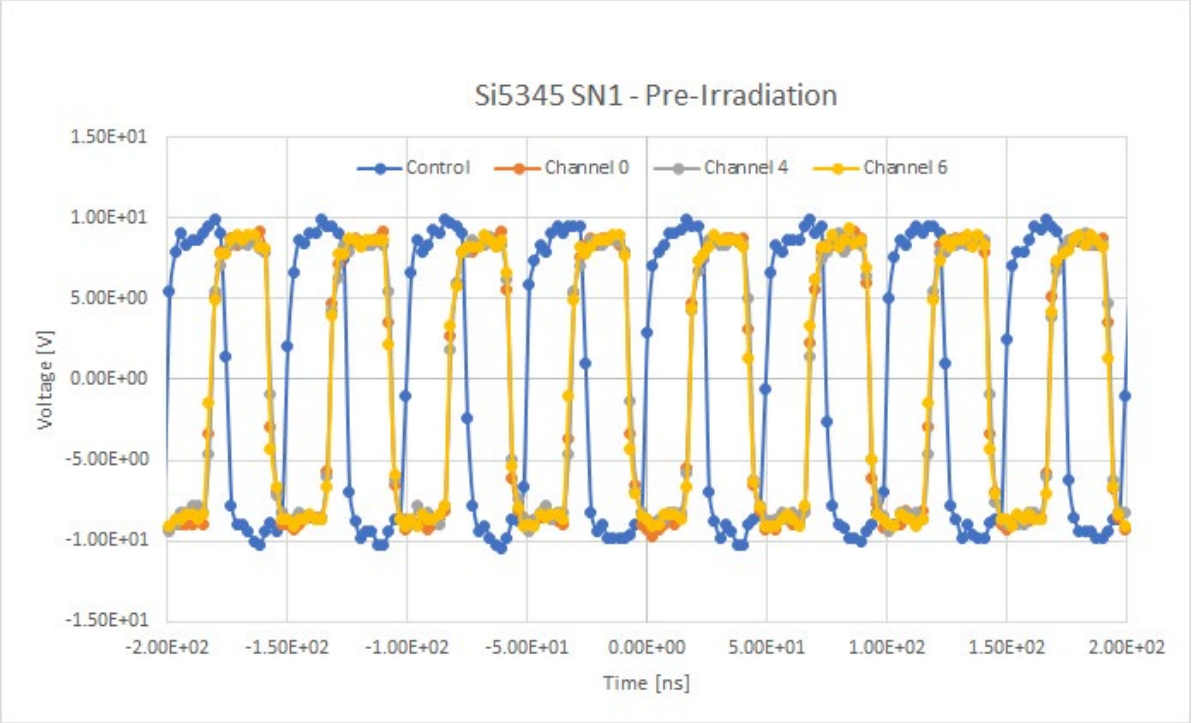

Figure 18: Si5345 output voltage waveforms for the pre-irradiation control (blue) and DUT 1. Note that the temporal offset of the control and DUT 1 waveforms is due to differences in cable lengths into the oscilloscope.

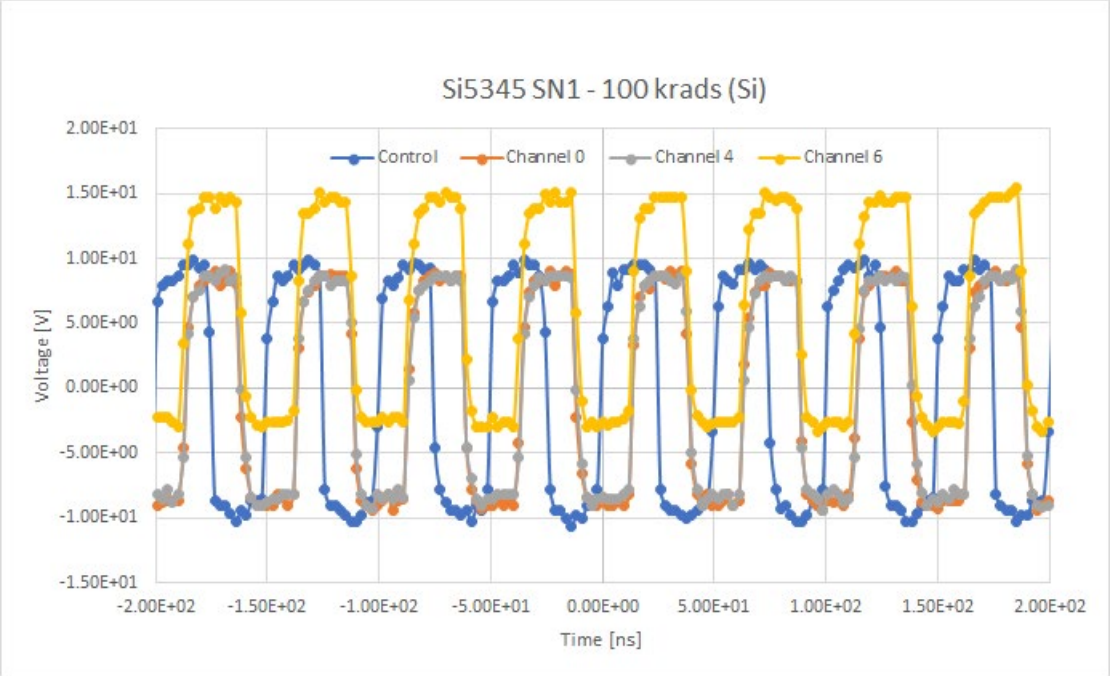

Figure 19: Si5345 output waveforms for the control (blue) and DUT 1 after 100 krad(Si). Note that the temporal offset of the control and output waveforms is due to differences in measurement configuration and the vertical offset from channel 6 is an erroneous oscilloscope setting.

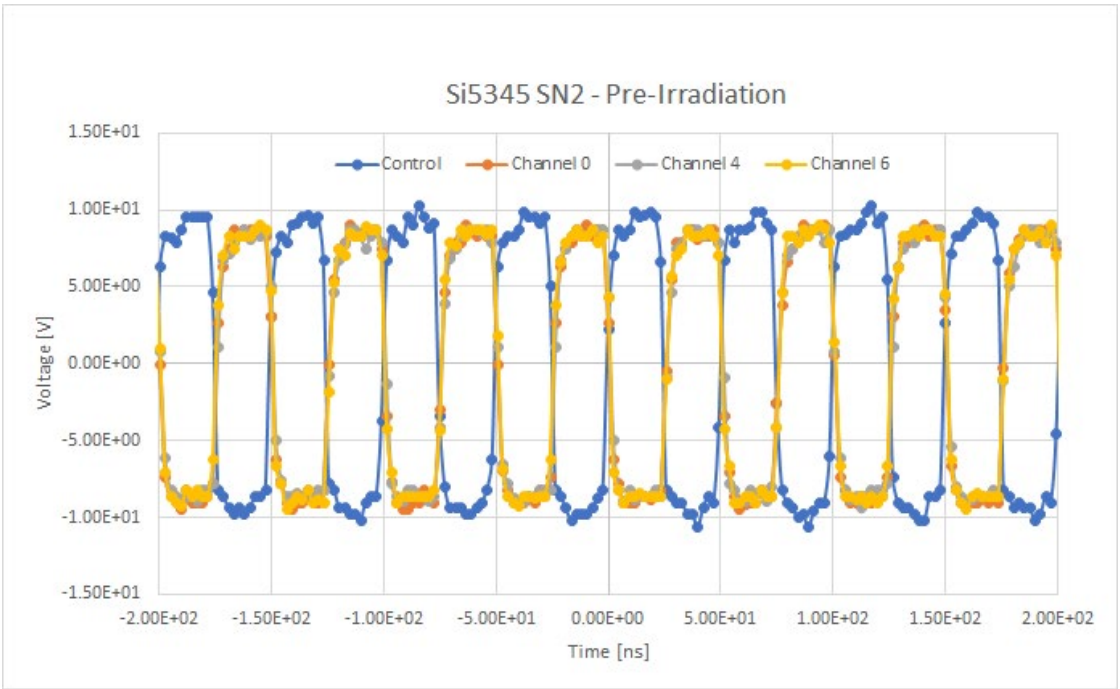

Figure 20: Si5345 output voltage waveforms for the pre-irradiation control (blue) and DUT 2. Note that the temporal offset of the control and output waveforms is due to differences in measurement configuration.

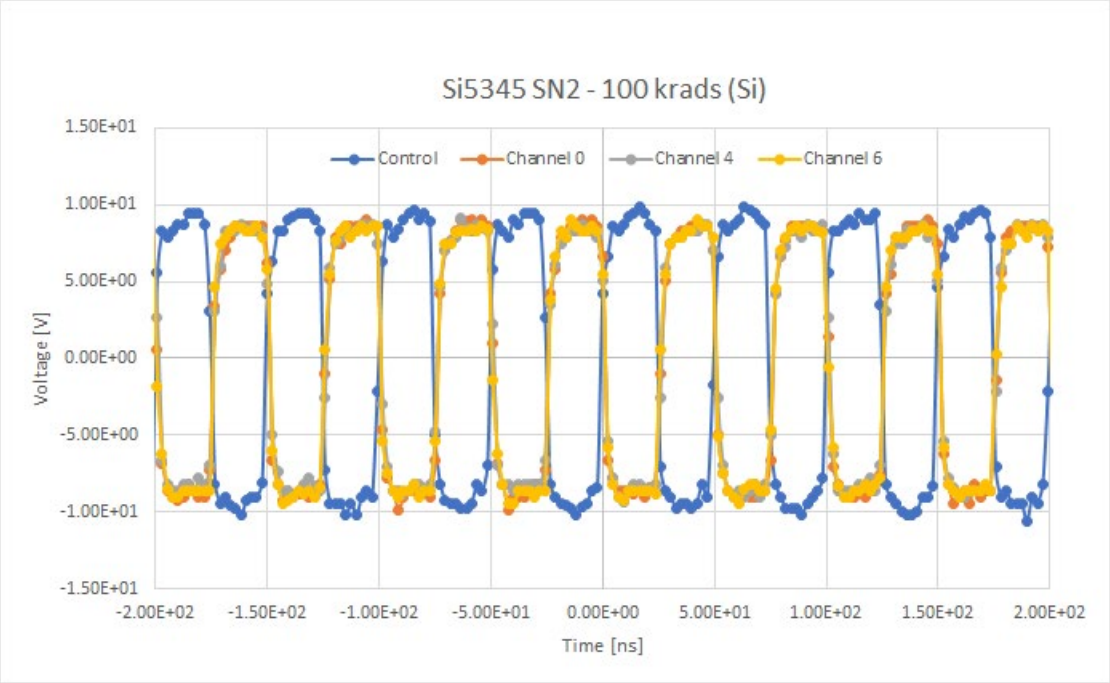

Figure 21: Si5345 output waveforms for the control (blue) and DUT 2 after 100 krad(Si). Note that the temporal offset of the control and output waveforms is due to differences in measurement configuration.

5.2. SY88422L

Three SY88422L devices (one control and two irradiated DUTs) were supplied with a 3.3 V bias to power the devices through the entirety of irradiation and measurements. A 10 ns signal with a repetition of 100 kHz was supplied as input waveform to each device using a function generator and the output waveform was monitored for any radiation-induced timing degradation using an oscilloscope that captured waveforms once every 20 seconds. It should be noted that both irradiated devices were supplied by the same function generator through 30 ft BNC cables while the control device was connected to a separate function generator using 6 ft BNC cables. The output of all three were monitored via the same oscilloscope, though the cabling length was equivalent to the function generator cabling.

Waveforms from all three devices are presented in Figures 22-26. Though there are temporal offsets of the control and irradiated waveforms, it can be seen that the duration of the output pulses remained consistent as a function of dose (10 ns durations are provided as a guide for the eye). It should be noted that the change in amplitude of the control pre-rad and post-2 krad(Si) measurement step is due to the addition of a 50 Ω terminator to the oscilloscope probe. There is some variability in the amplitude of one of the irradiated devices (denoted SN1), but as this variation was not monotonic it is attributed to an issue with the test harness. This theory can be further corroborated by the waveforms from the annealing phase of testing (Figure 27), which output consistent waveforms when tested outside of the chamber.

As the control and the irradiated devices were controlled by independent function generators, it is not practical to ascribe any significance to the temporal offset between the control and irradiated devices as the input waveforms were generated independently. Furthermore, because the control device was measured outside of the radiation chamber, it is reasonable to expect that the difference in cable length would result in a temporal offset in the waveforms during measurements of the control and irradiated devices. The impact of cabling length on the temporal offset of the waveforms can also explain the difference in offset of the control and irradiated waveforms from the annealing measurements (removing the irradiated devices from the chamber changed the cable length).

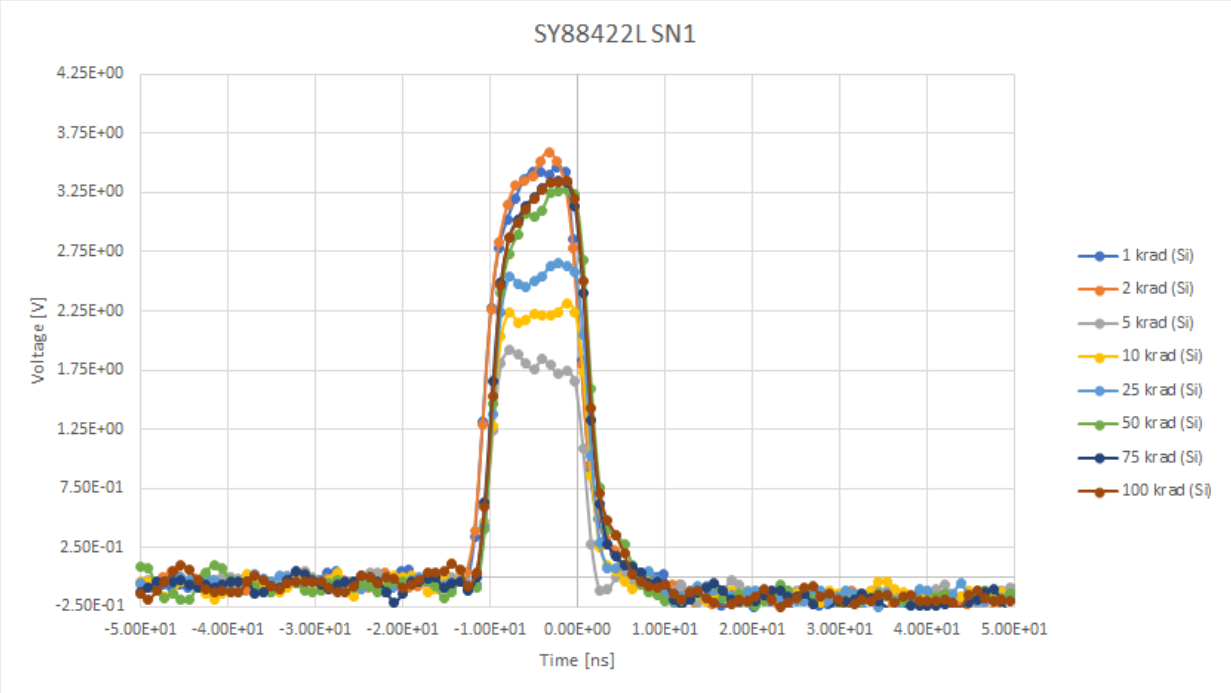

Figure 22: Waveforms as a function of dose for the SY88422L SN1 device. Note the temporary drop in amplitude observed at the 5,10, and 25 krad(Si) steps.

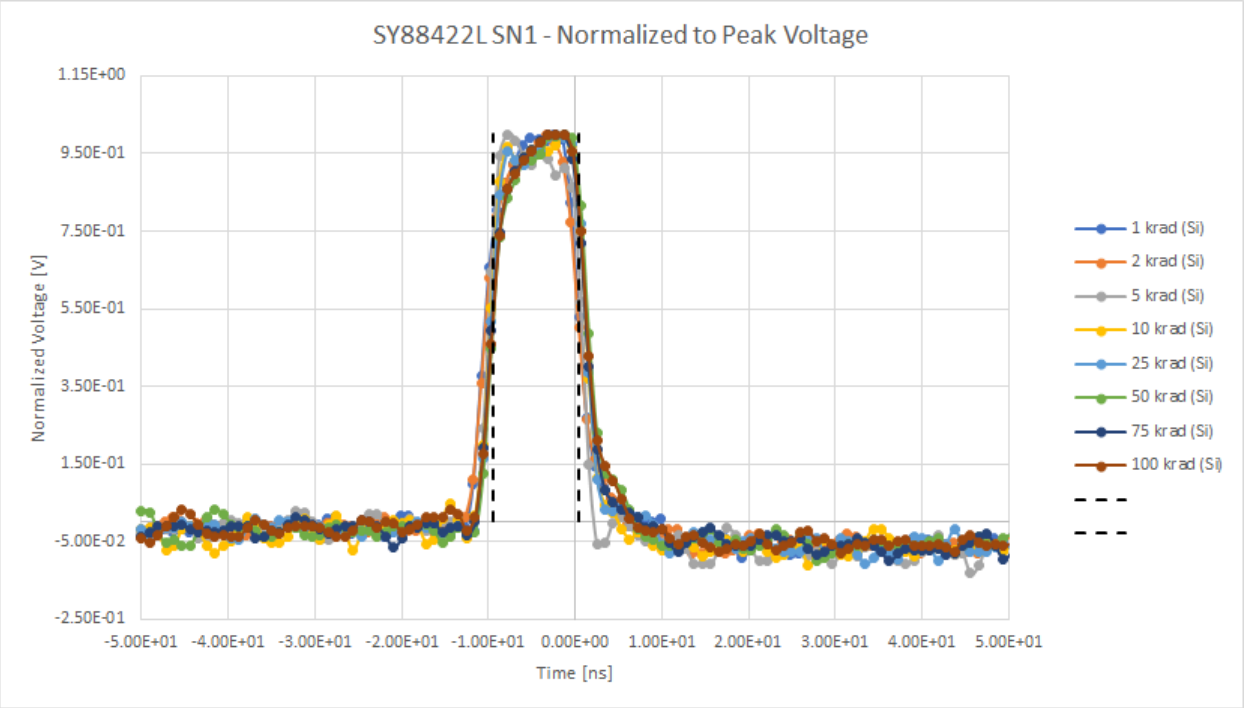

Figure 23: Waveforms normalized to peak voltage as a function of dose for the SY88422L SN1 device. The dashed lines denote a 10 ns duration.

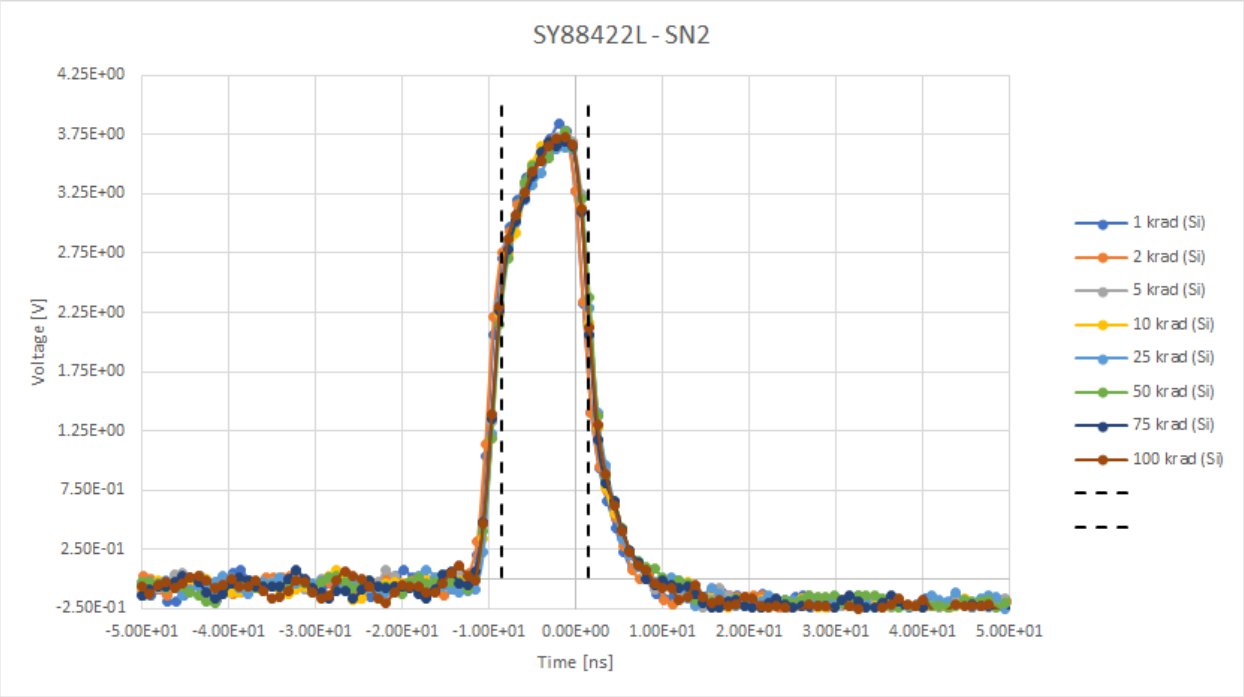

Figure 24: Waveforms as a function of dose for the SY88422L SN2 device. The dashed lines denote a 10 ns duration.

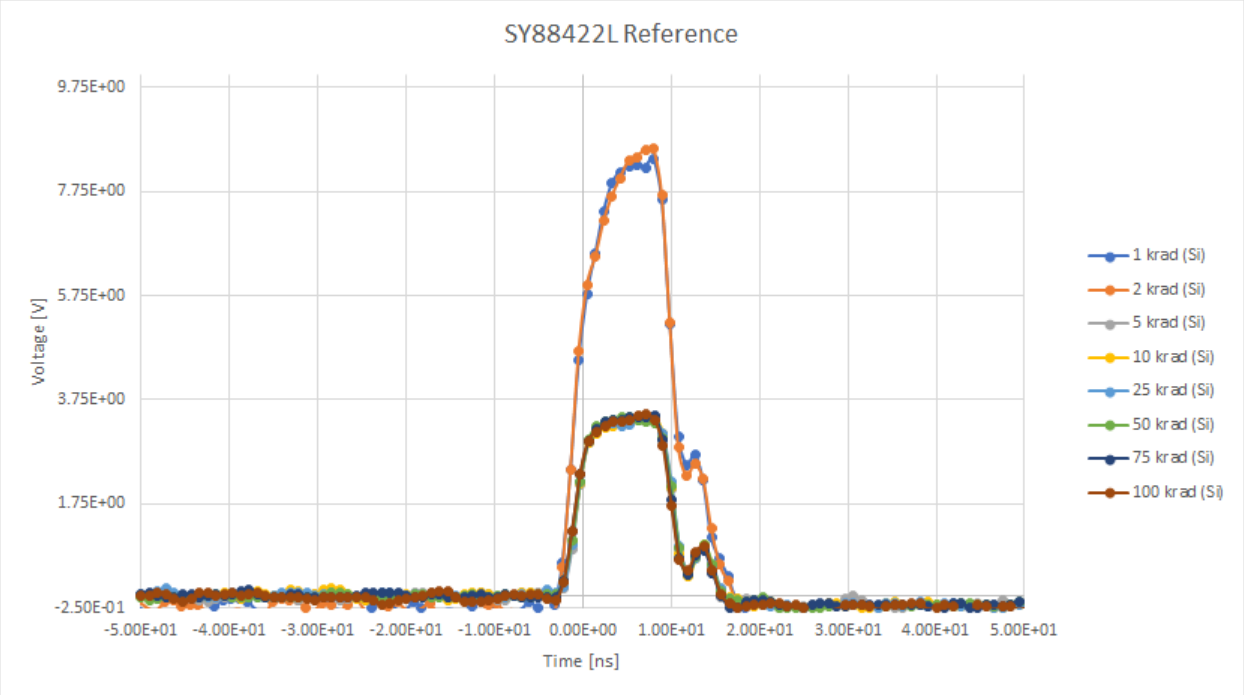

Figure 25: Waveforms as a function of dose for the SY88422L control device. The drop in amplitude following 2 krad(Si) dose step is due to the addition of a 50 Ω termination.

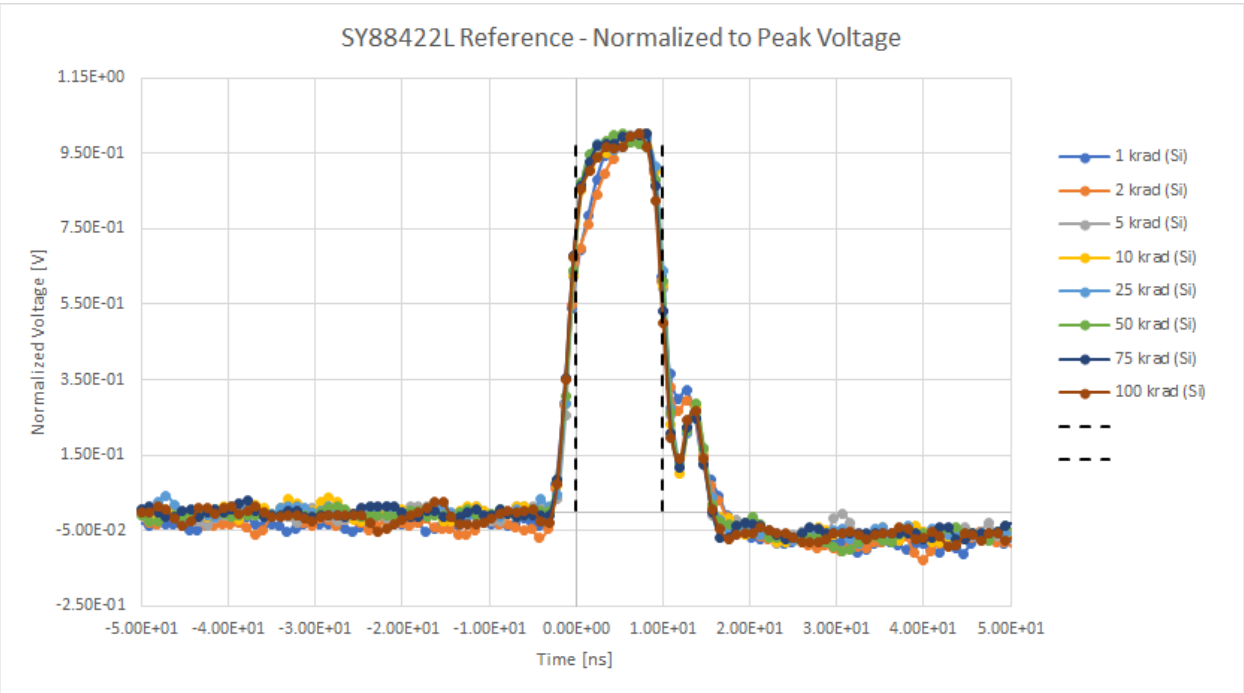

Figure 26: Waveforms normalized to peak voltage as a function of dose for the SY88422L control device. The dashed lines denote a 10 ns duration.

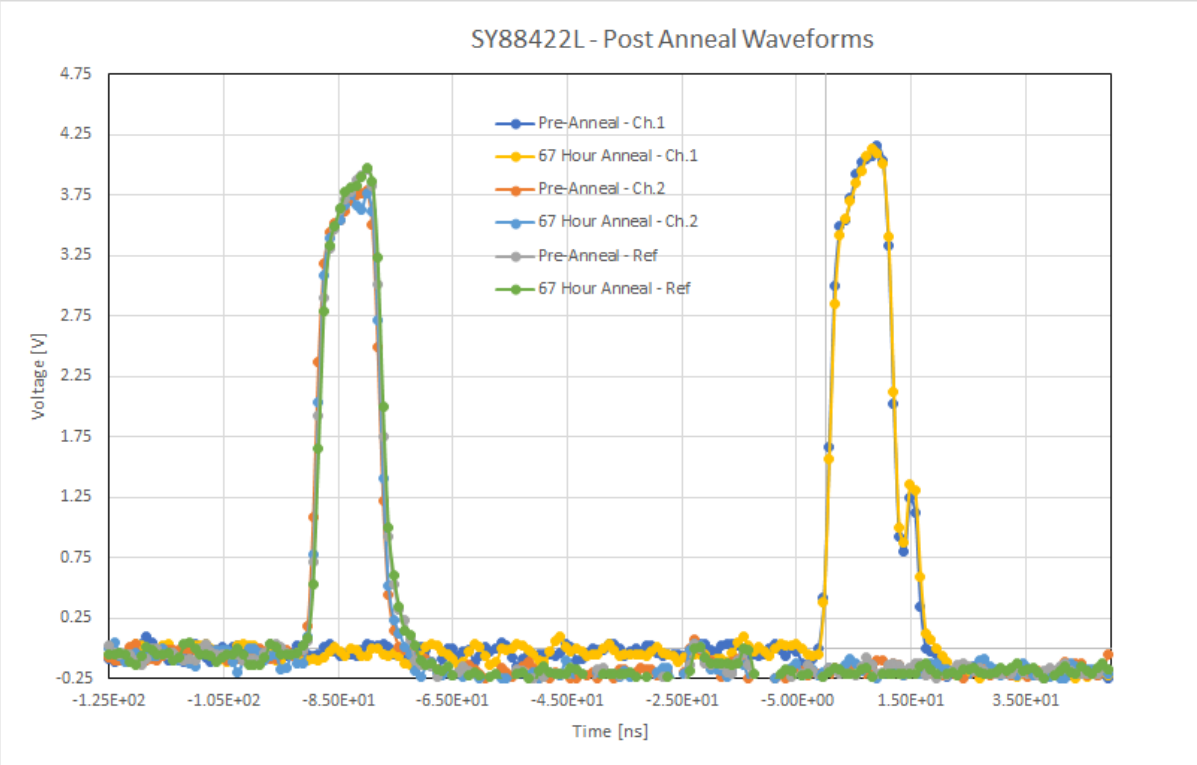

Figure 27: Pre- and post-anneal (67 hours) for SY88422L SN1-2 and the control devices. Note the temporal shift between the control and SN1-2 devices is a consequence of measurement configuration.

5.3. MSK130

Two power supplies (one at 80 V and another -15 V) were used to bias the device during irradiation; the second supply also provided a 2 V input signal. A simple voltage divider was used to reduce the output voltage of the device by a factor of 25. Voltage measurement plots presented in this report reflect this reduction. In addition to monitoring the output voltage, the current draw from the power supplies was monitored for any change in power consumption of the device during irradiation (Figures 28-29). Due to the high operating voltage of this device, the radiation-induced increase in current draw resulted in significant power dissipation. No thermal management was used for these devices and at 10 krad(Si), the device was powered off to avoid damaging test equipment. The device was permanently damaged and non-operational at this dose step. Because it was irradiated simultaneously with the LT3482, it was not removed from the chamber after being powered off. Irradiations continued unbiased to 100 krad(Si) after which the DUT was again characterized for current draw.

Figure 30 shows the output voltage as a function of dose up to 10 krad(Si). The output voltage decreases as a function of dose with a drop in output voltage of ~2 V (~2.5% decrease from nominal operation). In contrast, the current draw of the device as a function of dose shows a large, nearly 10x increase over the nominal current draw (Figures 28-29). As indicated previously, bias was removed and the DUT continued to be irradiated unbiased. Measurements immediately following the conclusion of 100 krad(Si) accumulated dose showed that under bias, the device drew current in excess of 500 mA.

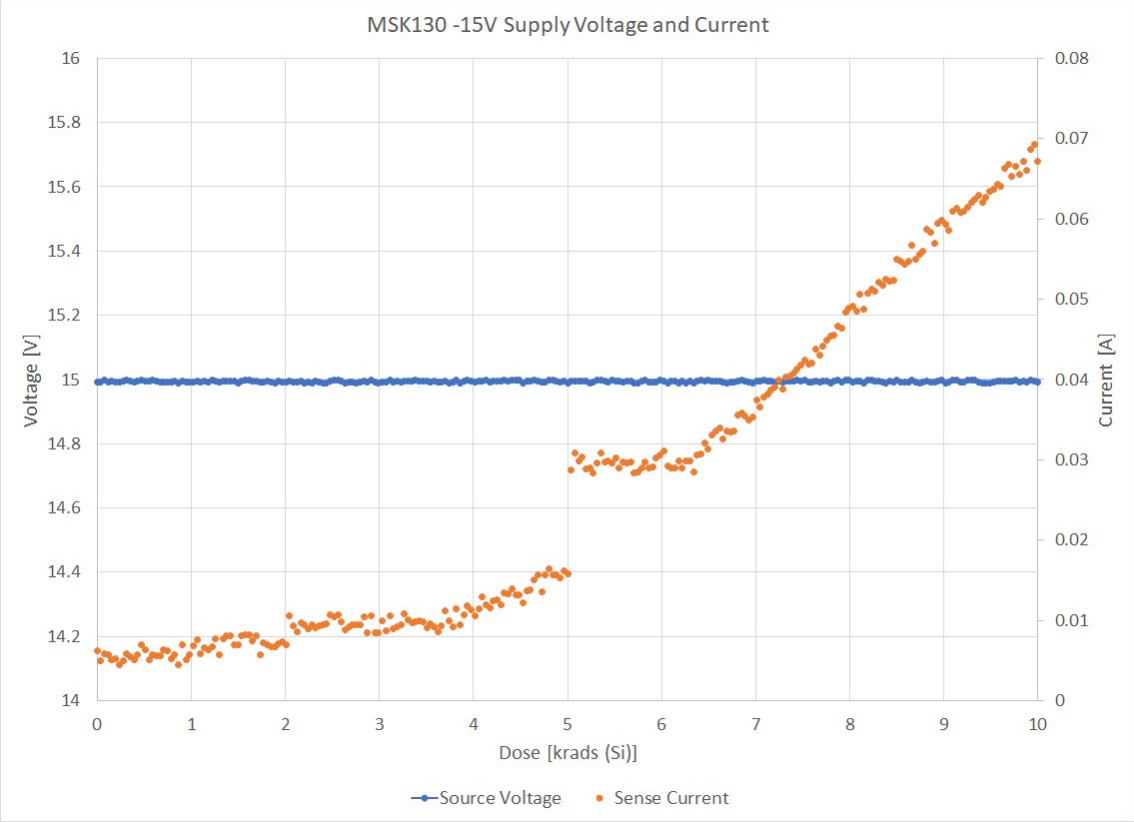

Figure 28: Voltage and current measurement of the –15V voltage supply as a function of dose for the MSK130 device.

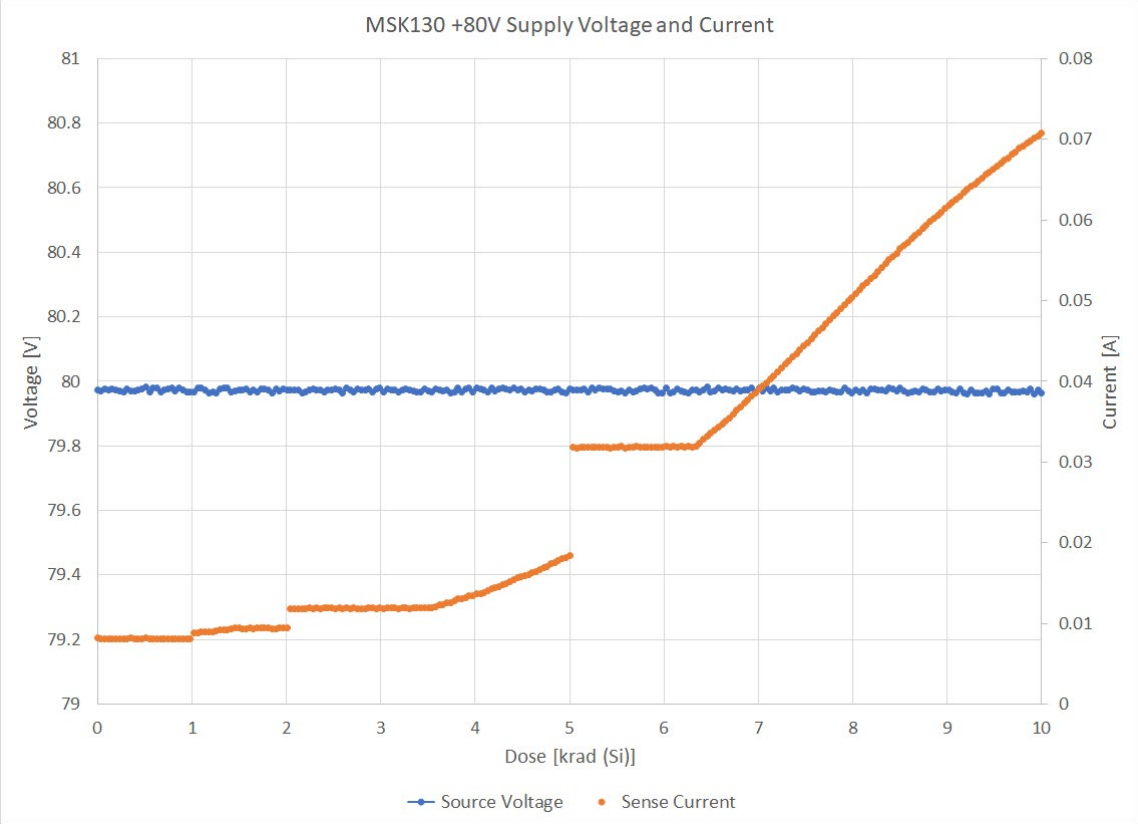

Figure 29: Voltage and current measurement of the 80V voltage supply as a function of dose for the MSK130 device.

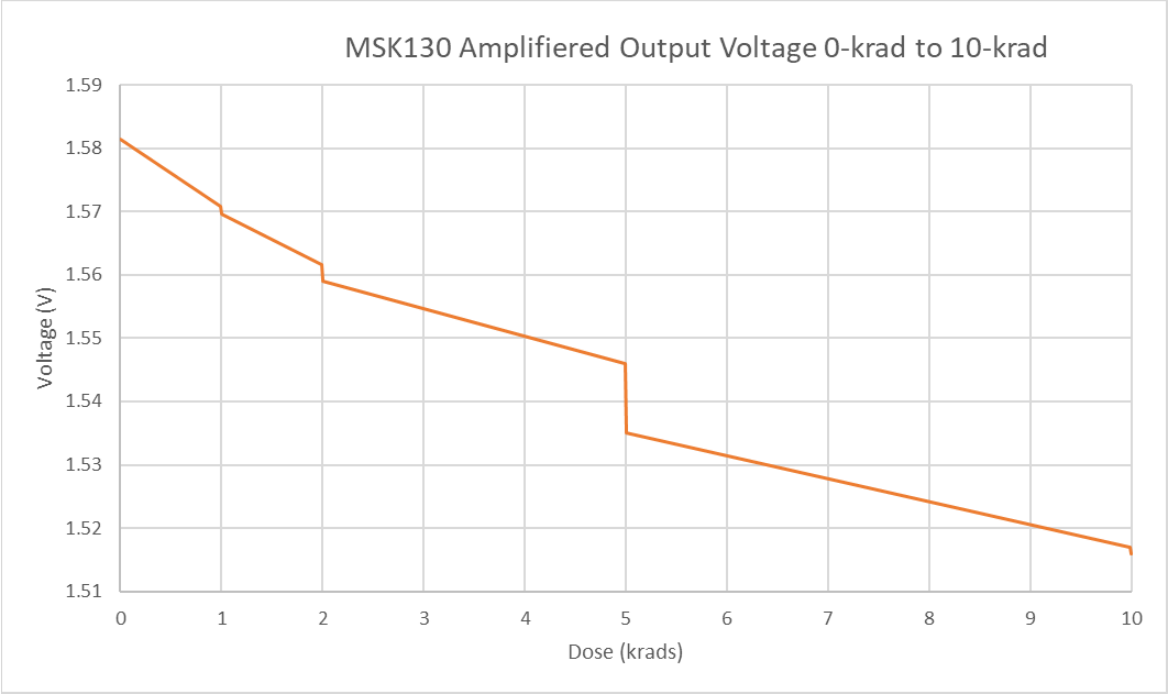

Figure 30: Output voltage of the 1:25 voltage divider as a function of dose for the MSK130 device.

5.4. LT3482

A 3.3 V input bias and 1 V control signal were applied to the LT3428 device from a single power supply. A simple voltage divider was used to reduce the output voltage of the device by a factor of 25 for the voltage measurements presented in this report. In addition to the output voltage, the power supply current draw was monitored for any radiation-induced change. The device was irradiated to a total dose of 100 krad(Si). It is important to note that though the LT3482 had distinct input/output channels it shared a power supply, was irradiated concurrently, and had its output voltage monitored with the same acquisition module as the MSK130 device. This concurrency is noteworthy as there is an abrupt shift in the output voltage at 10 krad(Si), corresponding to the powering off the MSK130 device

Figure 31 shows the power supply voltage and current output as a function of dose. The power supply voltage stays constant and the power supply current gradually decreases as a function of dose. A similar gradual decrease in the output voltage as a function of dose can be seen in Figure 32 though the abrupt shift at 10 krad(Si) complicates a quantitative analysis of the shift induced by a 100 krad(Si) total dose. Roughly bounding the shift from 10-100 krad(Si) corresponds to an output voltage shift of less than 0.5 V. As the power supply measurements remain are not perturbed by the removal of the MSK130 channel it is likely that the abrupt shift at 10 krad(Si) results from an issue with the output voltage current measurement system being shared with the MSK130 device, but a root cause was not identified.

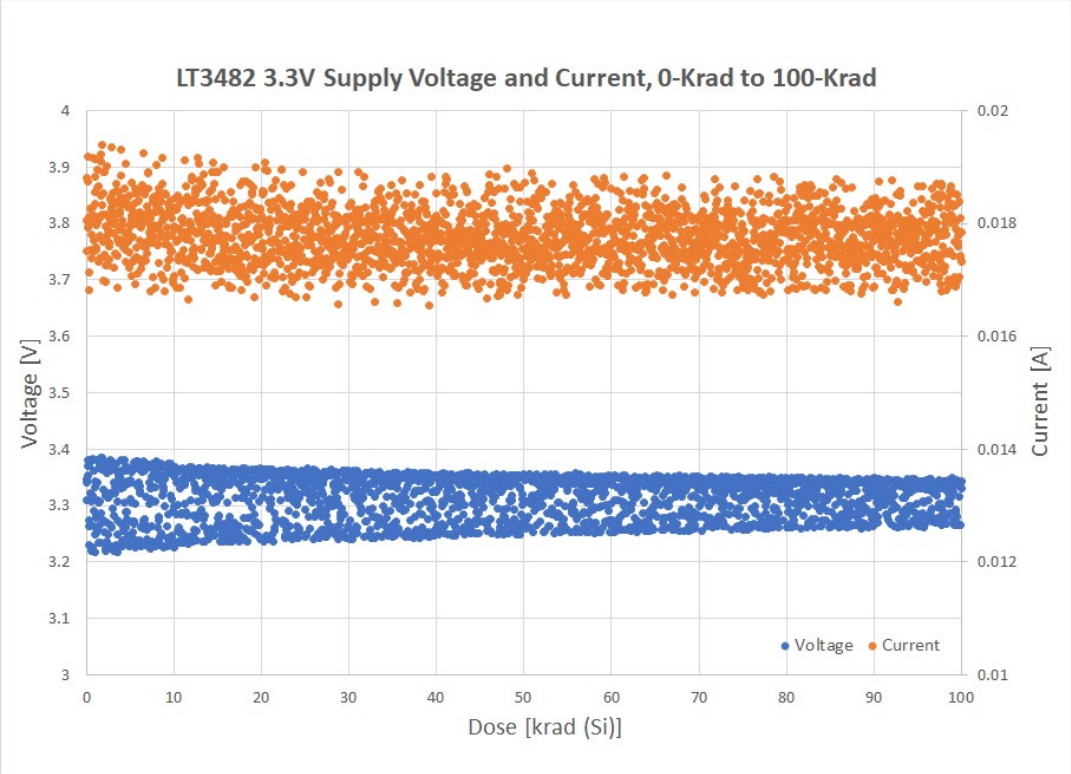

Figure 31: Voltage and current measurement of the 3.3 V voltage supply as a function of dose for the LT3482 device.

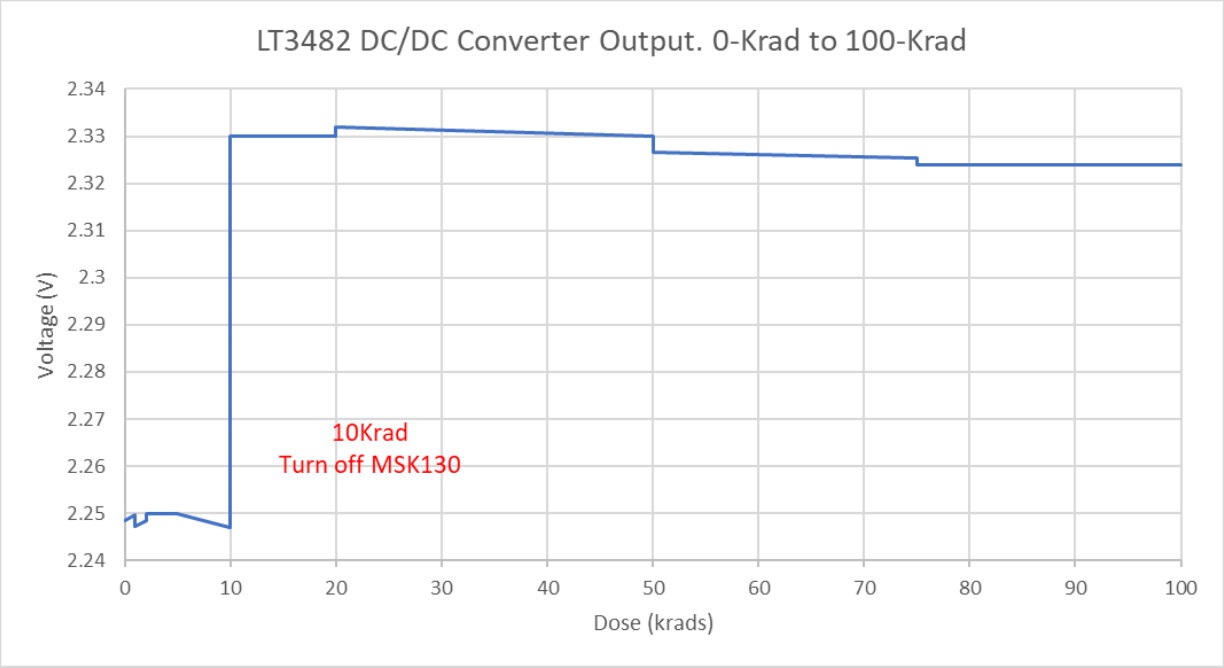

Figure 32: Output voltage of the 1:25 voltage divider as a function of dose for the LT3482 device. Note the abrupt change in voltage at the 10 krad(Si) dose step corresponds with the powering off of the MSK130 device that was being measured concurrently.

6. SUMMARY

Total ionizing dose characterization was performed with ~1 MeV gamma rays at high dose rate on a clock synthesizer (Si5345), laser driver (SY88422L), DC/DC converter (LT3482), and a high-speed amplifier (MSK130). Minimum degradation was observed in the timing performance of the Si5345 and SY88422L devices up to 100 krad(Si). The LT3482 displayed minimal change in the power consumption and output voltage up to a dose of 100 krad(Si). The MSK130 exhibited a significant increase (~10x) in power consumption as function of dose resulting in its testing being limited to 10 krad(Si).

This test campaign was designed to give an initial look at candidate parts. Extremely small sample sizes (1 and 2) and high dose rates (no ELDRS considerations) greatly limit the applicability of the test results. Part-to-part variability to ionizing dose can be significant in some devices, thus the results of these tests should be interpreted with care.

7. REFERENCES

1) SkyWorks, “Si5345/44/42 Rev D Data Sheet,” Accessed: Oct. 2021. [Online]. Available: https://www.skyworksinc.com/-/media/SkyWorks/SL/documents/public/data-sheets/si5345-44-42-d-datasheet.pdf
2) MicroChip, “4.25Gbps Laser Driver with Integrated Bias,” Accessed: July 2021. [Online]. Available: https://www.microchip.com/en-us/product/SY88422L
3) Analog Devices, “90V Boost DC/DC Converter with APD Current Monitor,” Accessed: July 2021. [Online]. Available: https://www.analog.com/media/en/technical-documentation/data-sheets/3482fa.pdf

4) TTM Technologies, “Ultra High Voltage High Speed Differential Op-Amp,” Accessed: July 2021. [Online]. Available: https://www.ttm.com/files/products/microelectronics/amplifiers/MSK130/MSK130_DataSheet%28Rev_f%29.pdf
5) Department of Defense “Test Method Standard Microcircuits,” MIL-STD-883 Test Method 1019.9 Ionizing radiation (total dose) test procedure, June 7, 2013, https://landandmaritimeapps.dla.mil/Downloads/MilSpec/Docs/MIL-STD-883/std883.pdf.